Visualization of Nucleosomal Substructure in Native Chromatin by Atomic Force Microscopy†

Linda D. Martin, James P. Vesenka, Eric Henderson, and Drena L. Dobbs*

Department of Zoology and Genetics, Signal Transduction Training Group, Iowa State University, Ames, Iowa 50011

Received November 4, 1994; Revised Manuscript Received January 30, 1995®

ABSTRACT: Intact rDNA minichromosomes from *Tetrahymena thermophila* were isolated as native chromatin and imaged by atomic force microscopy (AFM). AFM measurements of condensed rDNA chromatin were consistent with a 30 nm fiber that frequently (87% of molecules observed) contained stretches of nucleosome cores arranged in a zig-zag conformation. Examination of rDNA chromatin in a dispersed conformation by tapping mode AFM in low humidity resulted in high resolution images of partially dissociated nucleosome cores and associated linker DNA. A majority of these nucleosome cores contained six to eight smaller particles with dimensions consistent with those of individual histones. Many of the nucleosome cores showed a striking resemblance to the wedge (35%), axial (15%), and front (6%) views of the nucleosome histone octamer modeled by Arents *et al.* [Arents, G., Burlingame, R. W., Wang, B.-C., Love, W. E., & Moudrianakis, E. N. (1991) *Proc. Natl. Acad. Sci. U.S.A. 88,* 10148−10152]. This direct visualization of histone subunits and nucleosomal substructure in native chromatin illustrates the potential use of AFM to localize individual proteins in condensed cellular chromatin.

The structural organization of chromatin is fundamental to the replication, transmission, and expression of genetic information in eukaryotic cells. Although the location of core and linker histones relative to the path of the DNA in the nucleosome has been established (Baldwin *et al.*, 1975; Allan *et al.*, 1980; Richmond *et al.*, 1984; Arents *et al.*, 1991; Arents & Moudrianakis, 1993), the mechanisms by which nucleosomes become compacted into higher order structures have not yet been determined. Several alternative structures have been proposed for the 30 nm chromatin fiber thought to represent the primary level of chromatin folding (Finch & Klug, 1976; Belmont *et al.*, 1989; Wolffe, 1992). These include a solenoid model in which chromatin is organized into a cylinder with six nucleosomes per turn (Finch & Klug, 1976; Thoma *et al.*, 1979; McGhee *et al.*, 1980), a helical ribbon model in which chromatin assumes a zig-zag conformation resembling a helix of two rows of staggered nucleosomes (Worcel *et al.*, 1981; Woodcock *et al.*, 1984), and other models that take into account the variable length of linker DNA (McGhee *et al.*, 1983; Butler, 1984; Felsenfeld & McGhee, 1986; Lowary & Widom, 1989; Athey *et al.*, 1990; Woodcock *et al.*, 1993). Others have proposed that cellular chromatin is not found primarily in a single conformation, but in a variety of asymmetric conformations (Rattner & Hamkalo, 1979; Belmont *et al.*, 1987; Rykowski *et al.*, 1988; Zlatanova *et al.*, 1994), and that the structure of condensed chromatin *in situ* resembles a ribbon with a variable zig-zag pattern (Horowitz *et al.*, 1994).

The ability to visualize individual histones and non-histone proteins in native chromatin fibers could significantly enhance our understanding of chromatin architecture. While progress has been made in discerning the location of individual histones in native chromatin (Allan *et al.*, 1980; Thomas & Khabaza, 1980; Banchev *et al.*, 1990; Leuba *et al.*, 1993), it has not yet been possible to observe directly chromosomal proteins within higher order chromatin structures. Previous studies have shown that atomic force microscopy (AFM)[1] can be used to image native and reconstituted chromatin fibers in a "beads-on-a-string" conformation (Vesenka *et al.*, 1992b; Allen *et al.*, 1993; Fritzsche *et al.*, 1994). Here we demonstrate that AFM can also be used to characterize native chromatin in more condensed conformations [see also Zlatanova *et al.* (1994) and Leuba *et al.* (1994)] and report the development of spreading and imaging techniques that allow visualization of substructural features of nucleosomes within extended chromatin fibers. The number of discrete particles observed within partially dissociated nucleosome cores and their dimensions were consistent with their identification as individual histone monomers. Furthermore, the arrangements of these putative histones were consistent with modeled views of the histone octamer based on X-ray crystallography (Arents *et al.*, 1991; Arents & Moudrianakis, 1993).

MATERIALS AND METHODS

Isolation of Tetrahymena rDNA Chromatin. Tetrahymena rDNA chromatin was isolated from partially synchronized cells by a modification of the procedure of Borkhardt and Nielsen (1981). Minichromosomes were purified by sucrose gradient centrifugation and dialyzed against physiological buffer (10 mM Tris-HCl, pH 7.5, 140 mM KCl, 5 mM $MgCl_2$). The purity and integrity of chromatin preparations

† This work is supported by National Science Foundation Grant DIR 9113595 to the Signal Transduction Training Group at Iowa State University and by National Institutes of Health Grant GM41899 to D.L.D. This is journal paper no. 16140 of the Iowa Agriculture and Home Economics Experiment Station, Ames, IA, Project #3065.

* To whom correspondence should be addressed. Phone: 515-294-1112; Fax: 515-294-2876. E-mail: d_larson@molebio.iastate.edu.

® Abstract published in *Advance ACS Abstracts,* March 15, 1995.

[1] Abbreviations: AFM, atomic force microscopy; rRNA, ribosomal RNA; rDNA, ribosomal RNA genes.

0006-2960/95/0434-4610$09.00/0

were monitored by electron microscopy. Chromatin samples prepared for AFM imaging as described below were coated with platinum and rotary shadowed with carbon. Replicas were floated onto copper electron microscopic grids and examined using a JEOL JEM-100cxII electron microscope.

Atomic Force Microscopy of Chromatin. For AFM analysis, chromatin in physiological buffer was deposited on freshly cleaved mica, allowed to adsorb for 5 min at room temperature, rinsed with 1 mL of deionized water to remove excess salt, and dried with N_2 gas. Following initial scans, samples were dried in an oven at ~50 °C. Scans shown in Figures 1, 3, and 4, which are very similar to the initial scans, are from oven dried samples. All AFM samples were scanned in less than 10% relative humidity, achieved using a humidity chamber (Bioforce Lab, Ames, IA) perfused with dry N_2 gas. Contact mode images were obtained on a Nanoscope III AFM (Digital Instruments, Santa Barbara, CA), using oxide-etched silicon nitride tips [200 μm, tip radius 10−20 nm as determined using colloidal gold standards (Vesenka *et al.*, 1993a, 1994)] at scan speed 0.2 μm/s and sampling forces less than 5 nN. Tapping mode images (Zhong *et al.*, 1993) were obtained on a Nanoscope III with a multimode AFM, using Nanoprobe silicon tips (125 μm, tip radius 5−10 nm) at scan speed 1 μm/s.

Contour Length Measurements of rDNA Chromatin. The following calculation was performed to estimate the approximate contour length expected for a condensed rDNA minichromosome. Assuming 146 base pairs (bp) are wrapped around each nucleosome and an average of 24 bp of linker DNA adjoining two nucleosomes, the maximum number of nucleosomes per rDNA molecule (21 000 bp) can be calculated as 123 nucleosomes/rDNA molecule. If the maximum number of nucleosomes lie in a staggered zig-zag conformation, the length of a compacted rDNA molecule would be ~1.0 μm (similar to the 1.1 ± 0.4 μm observed). Similar values are obtained by assuming a 21 kb rDNA molecule would be compacted 6−9 times by assembly into nucleosomes. To obtain actual contour length measurements of the rDNA minichromosomes, TIFF files generated from AFM scans were analyzed using NIH Image 1.53. Only individual minichromosomes that were not in apparent contact with other minichromosomes were measured. Individual nucleosomes or dissociated histone octamers and small fragments (< 0.4 μm) were not measured.

RESULTS

AFM of Native rDNA Chromatin. The macronuclear rRNA genes (rDNA) of *Tetrahymena thermophila* are highly amplified as 21 kb linear palindromic minichromosomes (Yao, 1986; Kapler, 1993) which can be separated from bulk chromatin (Borkhardt & Nielsen, 1981; Higashinakagawa *et al.*, 1992). Samples of rDNA minichromosomes isolated as native chromatin were spread from physiological buffer onto freshly cleaved mica for AFM imaging. Typical images collected in two different modes are shown in Figure 1. In the recently developed tapping mode AFM (Figures 1A−G), reduced lateral forces result in better sample preservation and higher resolution images (Zhong *et al.*, 1993; Hansma *et al.*, 1993). For comparison, several images of the same sample collected using contact mode AFM are also shown (Figures 1H−J).

Upon imaging portions of the sample located near the center of the mica surface, individual rDNA chromatin fibers were observed in condensed conformations within a background of spherical structures (individual nucleosomes and occasional dissociated histone octamers, see below) (Figure 1). Contour length measurements yielded a mean minichromosome length of 1.1 ± 0.4 μm (n = 67), with a range of 0.4−2.2 μm. These measured contour lengths are consistent with an rDNA chromatin sample in which most intact minichromosomes are present in higher order conformations, with minor populations of broken molecules and full length molecules in more extended conformations. The most obvious higher order structures were regions of zig-zig conformation (arrows in Figure 1A) in which two rows of staggered nucleosomes were visible (see below).

AFM Measurements of Nucleosomes in Condensed Chromatin. Both tapping mode (Figures 1A−G) and contact mode scans (Figure 1H−J) of the condensed chromatin revealed arrays of spherical structures (nucleosomes) organized in chromatin fibers. These spherical structures were readily observed in every minichromosome (Figure 1A). The apparent mean width of these structures imaged in tapping mode AFM was 23.2 ± 4.5 nm (n = 118) (Figure 2A), compared with an average width of 31.2 ± 4.9 nm (n = 72) obtained in contact mode AFM images. When corrected for the exaggeration of image width in AFM as a function of the radius of curvature of the scanning tip (Keller, 1991; Allen *et al.*, 1992; Vesenka *et al.*, 1992a), these measurements are consistent with a maximum width of ~11 nm for each individual nucleosome. These values are similar to those obtained in previous contact mode AFM studies of chromatin fibers with the characteristic "beads-on-a-string" appearance: nucleosome cores assembled *in vitro* into chromatin fibers ranged from ~30 to 40 nm wide, with the smallest cores measuring 27 nm (Allen *et al.*, 1993); nucleosomes in native chicken chromatin measured 30 ± 3 nm wide (Vesenka *et al.*, 1992b).

The mean height of nucleosomes in condensed rDNA chromatin measured in tapping mode AFM was 4.3 ± 1.2 nm (n = 105) (Figure 2B). These values are also similar to those for nucleosomes assembled *in vitro* (2.5−6.0 nm) (Allen *et al.*, 1993) and to the height established for the short axis of a nucleosome by X-ray diffraction (5.7 nm) (Finch *et al.*, 1977) and neutron scattering (5.5−6.0 nm) (Suau *et al.*, 1977; Imai *et al.*, 1986).

Conformations of Nucleosomes in Condensed Minichromosomes. Taking into account tip convolution, the widths observed for rDNA minichromosomes were consistent with a 30 nm chromatin fiber (Finch & Klug, 1976; McGhee *et al.*, 1980; Thoma *et al.*, 1979; Suau *et al.*, 1979). It was not possible to definitively identify any extended regions of solenoidal structure (Finch & Klug, 1976); however, zig-zag-like conformations were seen frequently (Figure 1A−E,H) and occurred at least once in 87% of molecules examined (n = 52). Although most of the minichromosomes observed near the center of the mica were condensed, some were present in more extended conformations (Figure 1F,G). These extended molecules, nonetheless, exhibited regions of asymmetrically arranged nucleosomes and did not resemble "beads-on-a-string".

Nucleosomal Substructure Observed in Extended Chromatin. In contrast to chromatin near the center of the mica surface, most chromatin fibers located at the periphery of the substrate were reproducibly observed in extended conformations. This was presumably due to surface tension at the edge of the sample compounded by additional rinsing

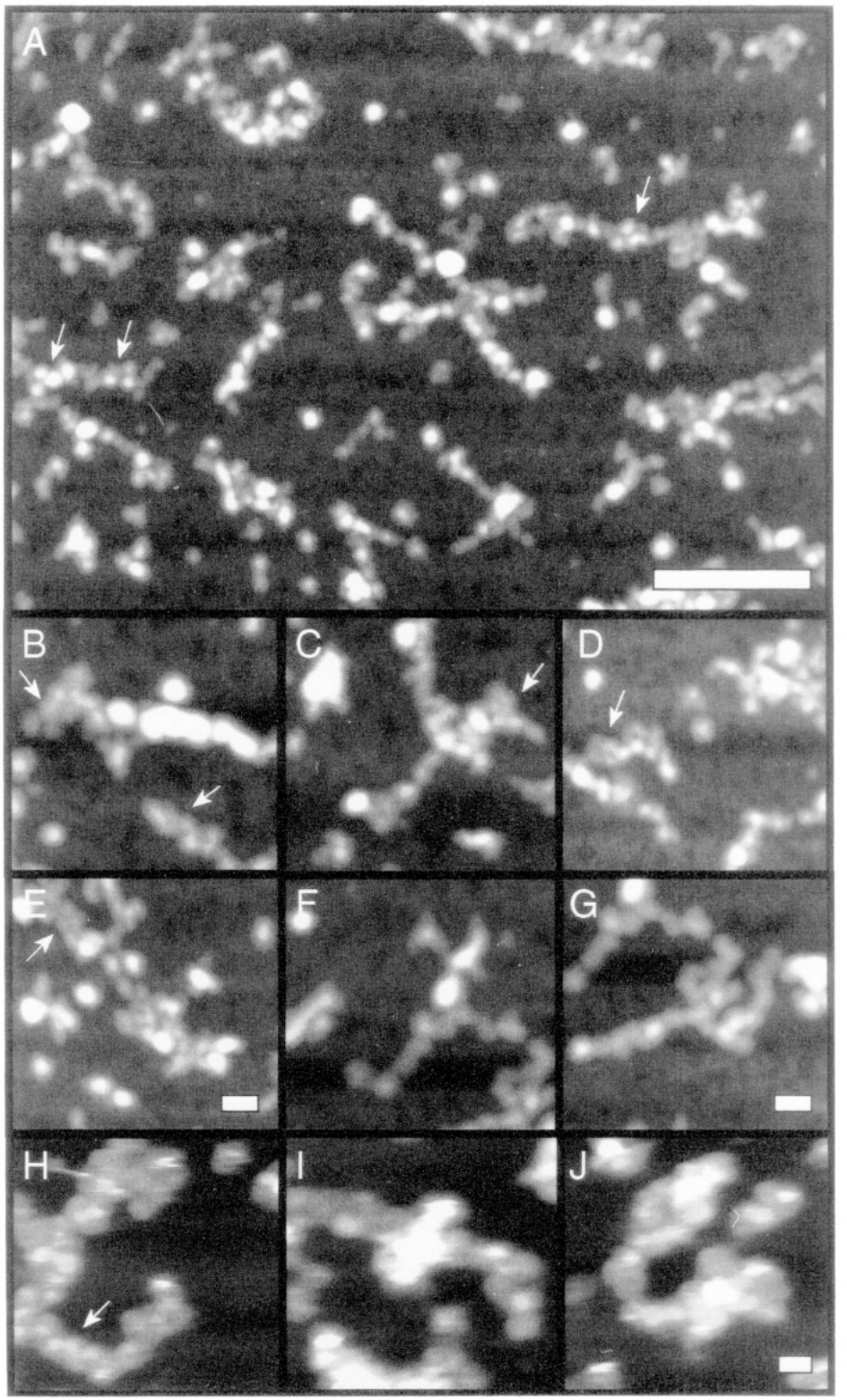

FIGURE 1: AFM images of condensed *Tetrahymena* rDNA minichromosomes. Native rDNA chromatin was isolated and prepared for AFM imaging on freshly cleaved mica. These images are representative of condensed chromatin found near the center of the mica surface in multiple samples from three different preparations. (A) A field of condensed rDNA chromatin imaged using tapping mode AFM. Arrows indicate some regions of nucleosomes in a zig-zag conformation. Scan size = 5.0 μm. Scale bar = 1 μm. (B−E) Tapping mode images of rDNA minichromosomes in which nucleosomes appear in a zig-zag pattern (see arrows). Scan size = 500 nm for panels B and C. 2× computer magnifications, shown in panels D and E, are from 1.28 μm scans. The vertical grayscale for these height mode images extends from 0 to 10 nm (black to white). Scale bars = 50 nm. (F−G) Tapping mode images of rDNA minichromosomes exhibiting other frequently observed conformations. Height grayscale same as for panels B−E. Scan size = 500 nm. Scale bar = 50 nm. (H−J) 2× computer magnifications of rDNA chromatin imaged in contact mode AFM. A region showing nucleosomes in a zig-zag conformation (see arrow) is shown in panel H. Panels I and J illustrate other typical views of condensed rDNA chromosomes. The vertical height grayscale extends from 0 to 15 nm (black to white). Scan size = 1.28 μm. Scale bar = 50 nm. Note that nucleosomes appear larger in contact mode images due to motion induced by the scanning tip (see text).

and drying forces. The more extended conformation facilitated visualization of structural features within and between individual nucleosomes (Figure 3A). In these tapping mode images, nucleosomes frequently appeared to have been

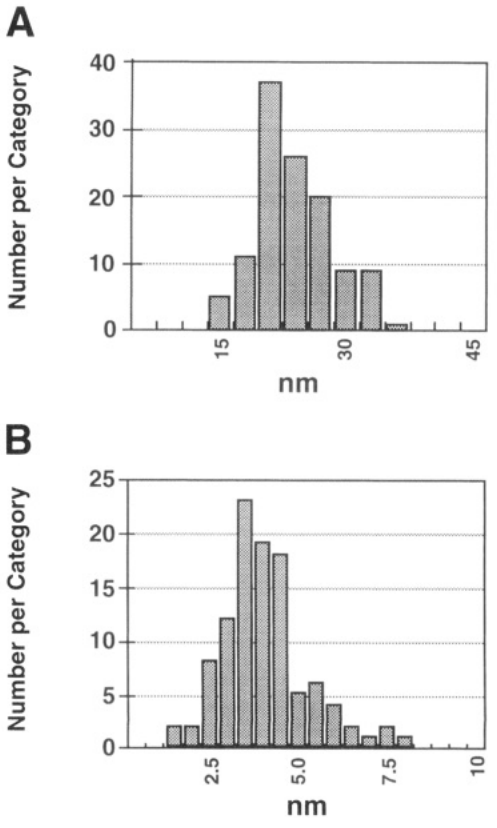

FIGURE 2: Histograms showing width and height distributions for nucleosomes in condensed rDNA chromatin imaged by tapping mode AFM. (A) Width of nucleosomes. The apparent mean width was 23.2 ± 4.5 nm (n = 118) with a range of 13.4−34.8 nm. (B) Height of nucleosomes. The apparent mean height was 4.3 ± 1.2 nm (n = 105) with a range from 1.9 to 8.1 nm.

partially dissociated, each composed of a cluster of smaller particles. From 4 to 9 smaller particles (mean = 6.7 ± 1.1, n = 47) per nucleosome were observed. The median number of particles per cluster was 8; 9% of the clusters contained 9 particles, but no clusters contained 10 or more particles. The mean width of the particles was 12.2 ± 3.1 nm (n = 82), and their mean height was 2.6 ± 0.8 nm (n = 93). These observations are consistent with the hypothesis that these smaller particles are individual histones (see Discussion).

Conformations of Nucleosomal Substructures. Many dissociated nucleosome cores (Figure 3) could be classified into three major structural categories which retained striking resemblances to three modeled views of the nucleosome octamer proposed by Arents *et al.* (1991), even though the nucleosomes had been partially dissociated. These conformations are also consistent with features of models proposed by other laboratories (Richmond *et al.*, 1984; Suau *et al.*, 1979). Of 204 cores examined, 35%, 15%, and 6% displayed the conformations shown in Figure 3 panels B, C and D, and E, respectively.

The first major structural category (Figure 3B) was very distinctive, with a high spot in the center of a butterfly-shaped cluster of spherical structures. This structural conformation resembled, both in shape and size, the wedge conformation proposed by Arents *et al.* (1991; Arents & Moudrianakis, 1993), in which a cylindrical wedge-shaped nucleosome is viewed with the widest part of the wedge lying on the substrate and DNA running perpendicular to the substrate. The highest point of this view measured 5.9 ± 1.3 nm (n = 72). This value is greater than the average nucleosome height observed in the condensed rDNA chromatin, 4.3 nm, where the nucleosomes are presumably viewed in an axial conformation (Arents *et al.*, 1991; Arents & Moudrianakis, 1993) with their shortest sides perpendicular to the substrate and their DNA lying parallel to the mica surface.

Nucleosomes in the second major structural category (Figure 3C,D) appeared essentially flat with approximately six particles visible, resembling the axial conformation. Nucleosomes in the third category (Figure 3E) appeared to have a diagonal raised ridge running across the core, resembling the front views illustrated by Arents *et al.* (1991). Cores in both the putative axial and front view categories had an average height of 4.4 ± 0.9 nm (n = 42), a value consistent with modeled views of the nucleosome and that observed for nucleosomes in the condensed minichromosomes. The remaining nucleosomes (44%) exhibited a variety of conformations (Figure 3F,G).

AFM of Nucleosomal DNA. In most orientations of nucleosomes, DNA was apparently wrapped around a core histone octamer parallel to the mica surface, making it difficult to resolve from the histones. Occasionally, however, fine linear connections between nucleosomes were observed. These structures were visible in height views of tapping mode images (Figure 4, left panels) but were more distinct in computer-generated illumination views of these scans (see arrows in Figure 4, right panels). The mean height of these structures was 0.9 nm, consistent with the height of double-stranded DNA previously measured by AFM (Bustamante *et al.*, 1992; Hansma *et al.*, 1992; Lindsay *et al.*, 1992; Vesenka *et al.*, 1992a; Yang *et al.*, 1992; Allen *et al.*, 1993; Shaiu *et al.*, 1993). Structures resembling DNA were only rarely associated with dissociated nucleosome cores, although fragments of DNA that appeared to have been sheared during sample preparation were frequently observed.

DISCUSSION

Individual nucleosomes in chromatin fibers organized in a "beads-on-a-string" conformation have been visualized previously by contact mode AFM (Vesenka, 1992b; Allen, 1993; Fritzsche et al., 1994; Zlatanova *et al.*, 1994). In this study, we have used tapping mode AFM (Zhong *et al.*, 1993) to examine the chromatin structure of isolated *Tetrahymena* rDNA minichromosomes in condensed, potentially native, conformations. Individual nucleosomes with dimensions similar to those reported in previous AFM studies were observed but were organized in more compact chromatin fibers. Moreover, the resolution obtained in these studies allowed direct visualization of individual histones within partially dissociated nucleosomes. The arrangements of these histone monomers within nucleosomes bore striking resemblance to modeled 3-D views of histone octamers determined by X-ray crystallography (Arents *et al.*, 1991; Arents & Moudrianakis, 1993).

Although the same substructural features were present in virtually all rDNA chromatin fibers from several rDNA minichromosome preparations, a variety of irregular chromatin conformations were observed. The most prominent ordered pattern consisted of regions of staggered nucleosomes in a zig-zag conformation arranged asymmetrically along individual chromosomes. Analogous asymmetric zig-zag structures have been reported for nuclear chromatin *in situ* (Horowitz, 1994) and are consistent with a helical ribbon model for the 30 nm chromatin fiber (Worcel, 1981; Woodcock, 1984). Alternative ordered conformations pre-

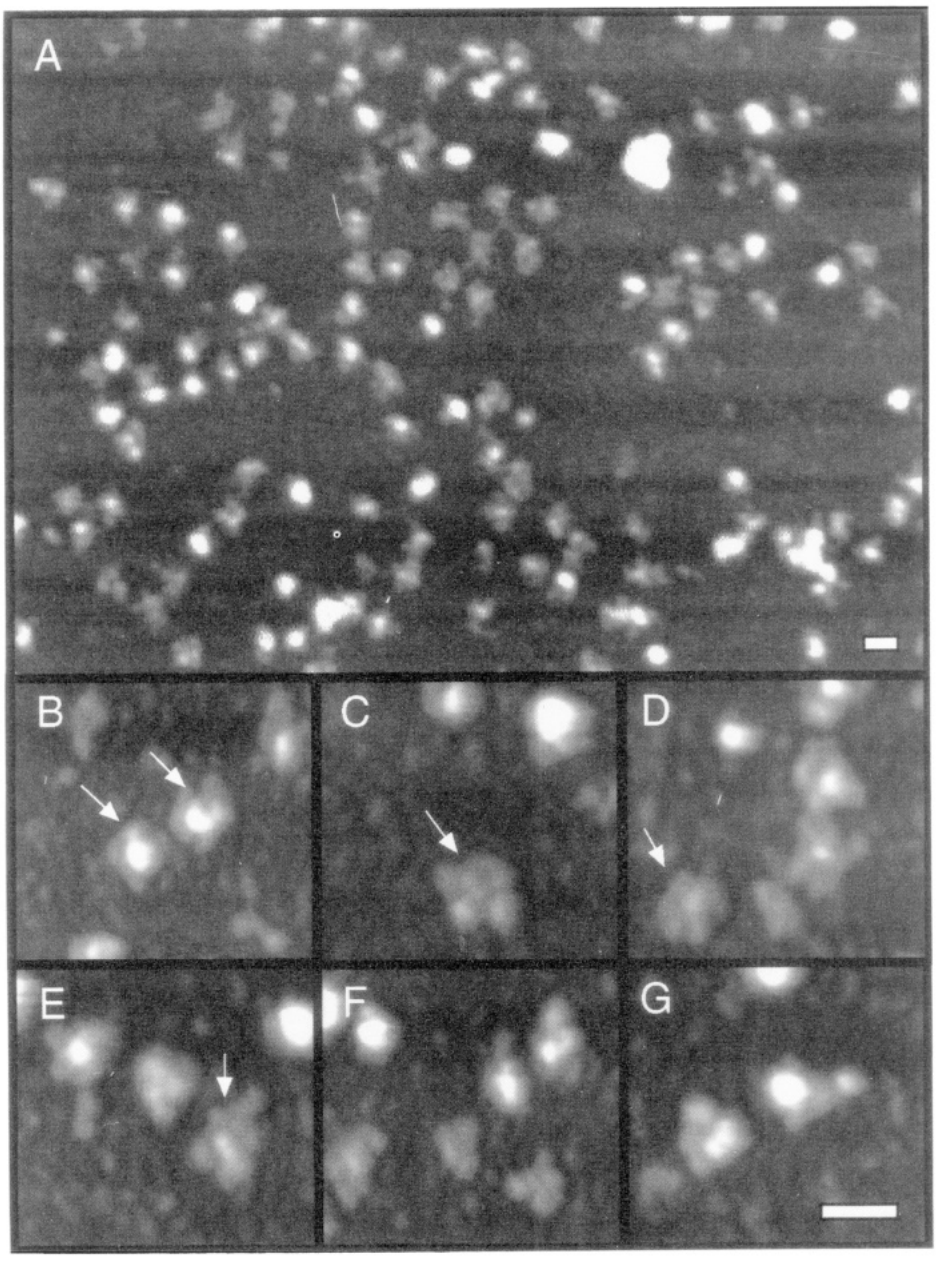

FIGURE 3: Images of extended rDNA chromatin illustrating structural features of partially dissociated nucleosomes. Tapping mode images shown here are from the periphery of the same sample shown in Figure 1. (A) Field in which individual nucleosomes have been partially dissociated. Scan size = 1.28 μm. Scale bar = 250 nm. (B−G) Views illustrating structural features reflecting the organization of individual histones within partially dissociated nucleosomes. Arrows in panels B, C and D, and E indicate repeated conformations observed in 35%, 15%, and 6% of the nucleosomes examined, respectively. Panels F and G show other structural conformations observed. These images are 2× computer magnifications of 1.28 μm tapping mode scans. Vertical grayscale for these height mode images extends from 0 to 15 nm (black to white). Scale bar = 50 nm.

dicted by other models for the 30 nm chromatin fiber such as solenoidal arrays were not observed. However, deposition of chromatin on a mica surface might compress solenoidal structures and distort their helical organization. Such conformational alterations have been observed in electron microscopic studies (Horowitz, 1994). It is also possible that the relatively short length of rDNA minichromosomes does not favor assembly of nucleosomes into solenoidal arrays. Finally, sample preparation and AFM scanning procedures may perturb native chromatin structures to some extent (see below). For whatever reason, in this study we did not observe structures consistent with a flattened solenoid containing six nucleosomes per turn with an 11 nm pitch (Finch & Klug, 1976).

In addition to information about the structural organization of condensed minichromosomes, tapping mode AFM provided striking views of substructural features of nucleosomes in extended chromatin fibers. First, clusters of 4−9 smaller spherical particles with dimensions expected for individual histone monomers were observed. The number of particles observed per nucleosome was consistent with partially dissociated core histone octamers, occasionally associated with linker histones. The absence of clusters with more than nine smaller particles is also consistent with this hypothesis. Second, more than 55% of the partially dissociated clusters corresponded to one of three modeled views of the core histone octamer based on X-ray crystallography (Arents *et al.*, 1991). The correspondence between these high resolution AFM images of chromatin and three-dimensional modeled views of the histone octamer based on X-ray crystallography at 3.1 Å resolution illustrates the potential of AFM as a new experimental approach for characterizing

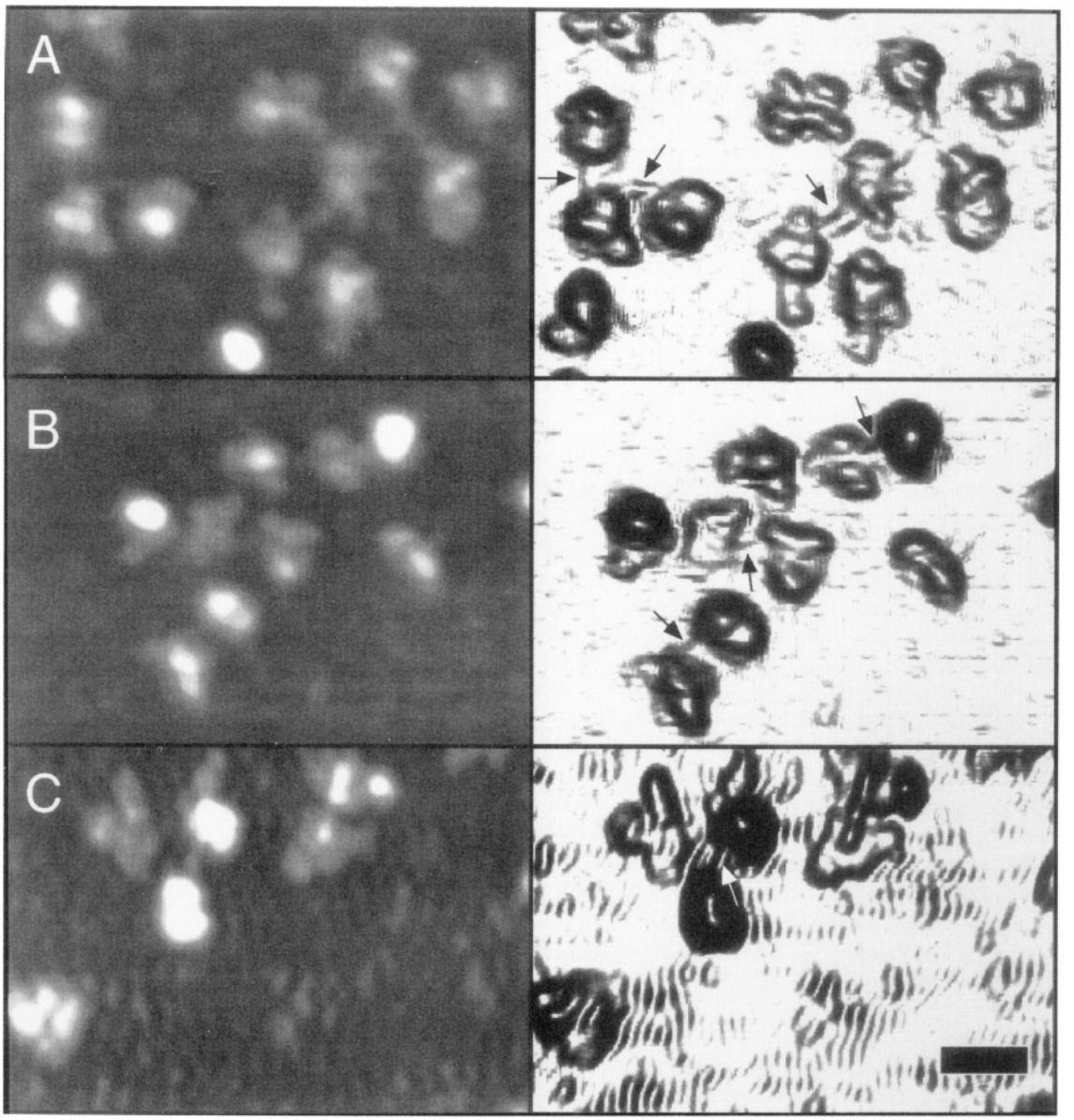

FIGURE 4: Tapping mode AFM images viewed in height (left panels) and illumination modes (right panels) illustrating linker DNA connecting nucleosomes. The illumination view accentuates edges of imaged structures so that structures such as DNA are readily visible. Arrows indicate linear structures with heights appropriate for double-stranded DNA. All panels show 2× magnifications of 1.28 μm scans. Panels A and B are enlargements of portions of Figure 3A. Panel C shows an image from an independent scan. Vertical grayscale for the height mode images extends from 0 to 9 nm (black to white). Scale bar = 50 nm.

the molecular structure of biological macromolecules.

Others have recently shown that tapping mode AFM can be used to examine the three-dimensional organization of extended chromatin fibers (Leuba *et al.*, 1994). Individual histone proteins within the nucleosome octamer were not resolved in that study or previous AFM studies (Vesenka *et al.*, 1992b; Allen *et al.*, 1993; Fritzsche et al., 1994). The higher resolution obtained in our study is likely due to the use of tapping mode AFM in low humidity. Previous work has shown that the salt layer surrounding AFM samples prepared in physiological buffers assumes fluid-like properties as it moves toward saturation with increasing humidity (Vesenka *et al.*, 1993b). Thus, particles are vulnerable to motion induced by the scanning tip which leads to image broadening and decreased resolution (Bustamante *et al.*, 1992; Thundat *et al.*, 1992; Vesenka *et al.*, 1993b). From this study, it appears that a decrease in humidity is necessary to reduce broadening and allow resolution of closely packed structures. This was achieved through humidity reduction in the atmosphere surrounding the sample. While cellular chromatin is in a more aqueous environment than that employed here, it has been shown that a 1 Å thick layer of water is present on mica in 10% humidity (Beaglehole & Christenson, 1992). Owing to the hygroscopic nature of residual buffer salts, it is likely that even more moisture resides around the chromatin, allowing for more physiologically relevant chromatin structures to be observed. Future AFM studies of chromatin in physiological saline should shed light on the effects of low humidity on structural characteristics.

The use of tapping mode AFM also results in images with more accurate widths than those obtained using contact mode AFM. This difference in tapping versus contact mode measurements is most likely attributable to sample motion in contact mode and reduced tip surface/sample contact in tapping mode (L.D.M., and J.P.V., unpublished data). The heights of the nucleosomes observed in condensed rDNA chromatin are consistent with the hypothesis that most nucleosomes contact the mica with their widest, presumably axial side down (i.e., the nucleosomes are lying such that

the DNA wrapped around them lies parallel to the mica surface). This is not surprising since surface tension is likely to promote maximal surface contacts. The reduced heights observed in this study could result in part from sample compression (Persson, 1987; Vesenka *et al.*, 1992b), which has been previously reported for flexible biomolecules subjected to loading forces typical of AFM scanning (Bustamante *et al.*, 1992; Vesenka *et al.*, 1993a).

We have shown that native rDNA chromatin from *T. thermophila* can be imaged by AFM in both condensed and extended conformations. Examination of partially dissociated nucleosome cores by tapping mode AFM in low humidity has revealed substructural features of nucleosome cores. The ability to resolve individual histones within nucleosomes by AFM suggests it will be possible to identify specific proteins in native chromatin structures by antibody labeling. Not only will the high resolution structural information obtained by AFM help elucidate chromatin structure but it should provide additional insight into the architecture of multiprotein complexes that catalyze DNA replication, transcription, and other fundamental cellular processes.

ACKNOWLEDGMENT

We thank R. M. Benbow and A. Myers for critical reading of the manuscript and T. C. Marsh for monitoring the rDNA chromatin preparation by electron microscopy.

REFERENCES

Allan, J., Hartman, P. G., Crane-Robinson, C., & Aviles, F. X. (1980) *Nature 288*, 675−679.
Allen, M. J., Hud, N., Balooch, M., Tench, R., Siekhaus, W., & Balhorn, R. (1992) *Ultramicroscopy 42−44*, 1095−1100.
Allen, M. J., Dong, X. F., O'Neill, T. E., Yau, P., Kowalczykowski, S. C., Gatewood, J., Balhorn, R., & Bradbury, E. M. (1993) *Biochemistry 32*, 8390−8396.
Arents, G., & Moudrianakis, E. N. (1993) *Proc. Natl. Acad. Sci. U.S.A. 90*, 10489−10493.
Arents, G., Burlingame, R. W., Wang, B.-C., Love, W. E., & Moudrianakis, E. N. (1991) *Proc. Natl. Acad. Sci. U.S.A. 88*, 10148−10152.
Athey, B. D., Smith, M. F., Rankert, D. A., Williams, S. P., & Langmore, J. P. (1990) *J. Cell Biol. 111*, 795−806.
Baldwin, J. P., Boseley, P. G., Bradbury, E. M., & Ibel, K. (1975) *Nature 253*, 245−249.
Banchev, T. B., Srebreva, L. N., & Zlatanova, J. S. (1990) *Mol. Cell. Biochem. 95*, 167−175.
Beaglehole, D., & Christenson, H. K. (1992) *J. Phys. Chem. 96*, 3395−3403.
Belmont, A. S., Sedat, J. W., & Agard, D. A. (1987) *J. Cell Biol. 105*, 77−92.
Belmont, A. S., Braunfeld, M. B., Sedat, J. W., & Agard, D. A. (1989) *Chromosoma 98*, 129−143.
Borkhardt, B., & Nielsen, O. F. (1981) *Chromosoma 84*, 131−143.
Bustamante, C., Vesenka, J., Tang, C. L., Rees, W., Guthold, M., & Keller, R. (1992) *Biochemistry 31*, 22−26.
Butler, P. J. G. (1984) *EMBO J. 3*, 2599−2604.
Felsenfeld, G., & McGhee, J. D. (1986) *Cell 44*, 375−377.
Finch, J. T., & Klug, A. (1976) *Proc. Natl. Acad. Sci. U.S.A. 73*, 1897−1901.
Finch, J. T., Lutter, L. C., Rhodes, D., Brown, R. S., Rushton, B., Levitt, M., & Klug, A. (1977) *Nature 269*, 29−36.
Fritzsche, W., Schaper, A., & Jovin, T. M. (1994) *Chromosoma 103*, 231−236.
Hansma, H. G., Vesenka, J., Siegerist, C., Kelderman, G., Morrett, H., Sinsheimer, R. L., Elings, V., Bustamante, C., & Hansma, P. K. (1992) *Science 256*, 1180−1184.
Hansma, H. G., Sinsheimer, R. L., Groppe, J., Bruice, T. C., Elings, V., Gurley, G., Magdalena, B., Mastrangelo, I. A., Hough, P. V. C., & Hansma, P. K. (1993) *Scanning 15*, 296−299.
Higashinakagawa, T., Narushima-Iio, M., Saiga, H., Kondo, S., & Mita, T. (1992) *Chromosoma 101*, 413−419.
Horowitz, R. A., Agard, D. A., Sedat, J. W., & Woodcock, C. L. (1994) *J. Cell Biol. 125*, 1−10.
Imai, B. S., Baldwin, J. P., Ibel, K., May, R. P., & Bradbury, E. M. (1986) *J. Biol. Chem. 261*, 8784−8792.
Kapler, G. (1993) *Curr. Opin. Genet. Dev. 3*, 730−735.
Keller, D. (1991) *Surf. Sci. 253*, 353−364.
Leuba, S. H., Zlatanova, J., & van Holde, K. (1993) *J. Mol. Biol. 229*, 917−929.
Leuba, S. H., Yang, G., Robert, C., van Holde, K., Zlatanova, J., & Bustamante, C. (1994) *Proc. Natl. Acad. Sci. U.S.A. 91*, 11621−11625.
Lindsay, S. M., Lyubchenko, Y. L., Gall, A. A., Shlyaktenko, L. S., & Harrington, R. E. (1992) *SPIE Proc. 1639*, 127.
Lowary, P. T., & Widom, J. (1989) *Proc. Natl. Acad. Sci. U.S.A. 86*, 8266−8270.
McGhee, J. D., Rau, D. C., Charney, E., & Felsenfeld, G. (1980) *Cell 22*, 87−96.
McGhee, J. D., Nickol, J. M., Felsenfeld, G., & Rau, D. C. (1983) *Cell 33*, 831−841.
Persson, B. N. J. (1987) *Chem. Phys. Lett. 141*, 366−368.
Rattner, J. B., & Hamkalo, B. A. (1979) *J. Cell Biol. 81*, 453−457.
Richmond, T. J., Finch, J. T., Rushton, B., Rhodes, D., & Klug, A. (1984) *Nature 311*, 532−537.
Rykowski, G. M., Parmelee, S. J., Agard, D. A., & Sedat, J. W. (1988) *Cell 54*, 461−472.
Shaiu, W.-L., Vesenka, J., Jondle, D., Henderson, E., & Larson, D. D. (1993) *J. Vac. Sci. Technol. A 11*, 820−832.
Suau, P., Kneale, G. G., Braddock, G. W., Baldwin, J. P., & Bradbury, E. M. (1977) *Nucleic Acids Res. 4*, 3769−3786.
Suau, P., Bradbury, E. M., & Baldwin, J. P. (1979) *J. Biochem. (Tokyo) 97*, 593−602.
Thoma, F., Koller, T., & Klug, A. (1979) *J. Cell Biol. 83*, 403−427.
Thomas, J. O., & Khabaza, J. A. (1980) *Eur. J. Biochem. 112*, 501−511.
Vesenka, J., Guthold, M., Tang, C. L., Keller, D., Delaine, E., & Bustamante, C. (1992a) *Ultramicroscopy 42−44*, 1243−1249.
Vesenka, J., Hansma, H., Siegerist, C., Siligardi, G., Schabtach, E., & Bustamante, C. J. (1992b) *SPIE Proc. 1639*, 127−137.
Vesenka, J., Manne, S., Giberson, R., Marsh, T., & Henderson, E. (1993a) *Biophys. J. 65*, 992−997.
Vesenka, J., Manne, S., Yang, G., Bustamante, C. J., & Henderson, E. (1993b) *Scanning Microsc. 7*, 781−788.
Vesenka, J., Miller, R., & Henderson, E. (1994) *Rev. Sci. Instrum. 65*, 2249−2251.
Wolffe, A. (1992) *Chromatin: Structure and Function*, Academic Press, New York.
Woodcock, C. L. F., Frado, L.-L. Y., & Rattner, J. B. (1984) *J. Cell Biol. 99*, 42−52.
Woodcock, C. L., Grigoryev, S A., Horowitz, R. A., & Whitaker, N. (1993) *Proc. Natl. Acad. Sci. U.S.A. 90*, 9021−9025.
Worcel, A., Strogatz, S., & Riley, D. (1981) *Proc. Natl. Acad. Sci. U.S.A. 78*, 1461−1465.
Yang, J., Takeyasu, K., & Shao, Z. (1992) *FEBS Lett. 301*, 173−176.
Yao, M.-C. (1986) in *The Molecular Biology of Ciliated Protozoa* (Gall, J. G., Ed.) pp 179−198, Academic Press, Inc., New York.
Zhong, Q., Inniss, D., Kjoller, K., & Elings, V. B. (1993) *Surf. Sci. Lett. 290*, L688−L692.
Zlatanova, J., Leuba, S. H., Yang, G., Bustamante, C., & van Holde, K. (1994) *Proc. Natl. Acad. Sci. U.S.A. 91*, 5277−5280.

BI942580G